

# Anterior thalamic nuclei deep brain stimulation inhibits mossy fiber sprouting via 3',5'-cyclic adenosine monophosphate/protein kinase A signaling pathway in a chronic epileptic monkey model

Ting-Ting Du<sup>1</sup>, Ying-Chuan Chen<sup>2</sup>, Guan-Yu Zhu<sup>2</sup>, De-Feng Liu<sup>2</sup>, Yu-Ye Liu<sup>2</sup>, Tian-Shuo Yuan<sup>2</sup>, Xin Zhang<sup>1</sup>, Jian-Guo Zhang<sup>2,3</sup>

<sup>1</sup>Department of Functional Neurosurgery, Beijing Neurosurgical Institute, Capital Medical University, Beijing 100070, China;

<sup>2</sup>Department of Neurosurgery, Beijing Tiantan Hospital, Capital Medical University, Beijing 100070, China;

<sup>3</sup>Beijing Key Laboratory of Neurostimulation, Beijing 100070, China.

## Abstract

**Background:** Anterior thalamic nuclei (ATN) deep brain stimulation (DBS) is an effective method of controlling epilepsy, especially temporal lobe epilepsy. Mossy fiber sprouting (MFS) plays an indispensable role in the pathogenesis and progression of epilepsy, but the effect of ATN-DBS on MFS in the chronic stage of epilepsy and the potential underlying mechanisms are unknown. This study aimed to investigate the effect of ATN-DBS on MFS, as well as potential signaling pathways by a kainic acid (KA)-induced epileptic model.

**Methods:** Twenty-four rhesus monkeys were randomly assigned to control, epilepsy (EP), EP-sham-DBS, and EP-DBS groups. KA was injected to establish the chronic epileptic model. The left ATN was implanted with a DBS lead and stimulated for 8 weeks. Enzyme-linked immunosorbent assay, Western blotting, and immunofluorescence staining were used to evaluate MFS and levels of potential molecular mediators in the hippocampus. One-way analysis of variance, followed by the Tukey *post hoc* correction, was used to analyze the statistical significance of differences among multiple groups.

**Results:** ATN-DBS is found to significantly reduce seizure frequency in the chronic stage of epilepsy. The number of ectopic granule cells was reduced in monkeys that received ATN stimulation ( $P < 0.0001$ ). Levels of 3',5'-cyclic adenosine monophosphate (cAMP) and protein kinase A (PKA) in the hippocampus, together with Akt phosphorylation, were noticeably reduced in monkeys that received ATN stimulation ( $P = 0.0030$  and  $P = 0.0001$ , respectively). ATN-DBS also significantly reduced MFS scores in the hippocampal dentate gyrus and CA3 sub-regions (all  $P < 0.0001$ ).

**Conclusion:** ATN-DBS is shown to down-regulate the cAMP/PKA signaling pathway and Akt phosphorylation and to reduce the number of ectopic granule cells, which may be associated with the reduced MFS in chronic epilepsy. The study provides further insights into the mechanism by which ATN-DBS reduces epileptic seizures.

**Keywords:** Anterior thalamic nuclei; Deep brain stimulation; Epilepsy; Hippocampus; Mossy fiber sprouting

## Introduction

Epilepsy is a common neurological disorder that affects 0.5% to 1% of the population worldwide,<sup>[1]</sup> and almost 30% of patients are refractory to existing medicines.<sup>[2]</sup> Not all patients with drug-resistant epilepsy are, however, suitable candidates for resective surgery, especially those with multiple seizure foci, seizure foci that are hard to locate, or seizure foci in brain regions where damage could lead to severe functional deficits.<sup>[3]</sup>

Deep brain stimulation (DBS) is a novel technique for neuromodulation that has recently been used in epilepsy patients who are unsuitable for resective surgery. Because

of its crucial role in seizure spread and the Papez circuit, the anterior thalamic nuclei (ATN) is regarded as one of the best targets for controlling seizures.<sup>[4]</sup> A double-blind, randomized, multicenter study found that treatment with ATN-DBS produced a median percentage seizure reduction from baseline of 41% in the first year and 69% in the fifth year. Better seizure control was achieved in patients with temporal lobe epilepsy (TLE, median percentage seizure reductions: 44% at 1 year and 76% at 5 years).<sup>[4]</sup>

Mossy fiber sprouting (MFS), a common pathological hallmark of TLE, could mediate reverberating excitation, which reduces the threshold for granule cell synchronization and plays a crucial role in the epileptic brain and

## Access this article online

Quick Response Code:



Website:

www.cmj.org

DOI:

10.1097/CM9.0000000000001302

Ting-Ting Du and Ying-Chuan Chen contributed equally to the present work.

**Correspondence to:** Jian-Guo Zhang, Neurosurgery Department, Beijing Tiantan Hospital, South Four Ring West Road No. 119, B District, Fengtai Dist, Beijing 100070, China  
E-Mail: zjguo73@126.com

Copyright © 2021 The Chinese Medical Association, produced by Wolters Kluwer, Inc. under the CC-BY-NC-ND license. This is an open access article distributed under the terms of the Creative Commons Attribution-Non Commercial-No Derivatives License 4.0 (CCBY-NC-ND), where it is permissible to download and share the work provided it is properly cited. The work cannot be changed in any way or used commercially without permission from the journal.

Chinese Medical Journal 2021;134(3)

Received: 19-10-2020 Edited by: Ning-Ning Wang

behavioral seizures.<sup>[5]</sup> MFS is regulated by multiple signaling pathways, among which 3',5'-cyclic adenosine monophosphate (cAMP)/protein kinase A (PKA) appears to play a particularly important role. Ectopic granule cells are also closely associated with MFS in epilepsy.<sup>[6]</sup> Although epileptogenesis in animal models is a continuous process, it can be divided into three stages: acute, latent, and chronic.<sup>[7]</sup> Clinically, almost all patients undergo ATN-DBS several years after the onset of epilepsy,<sup>[4]</sup> which corresponds to the chronic stage in animal models.<sup>[7]</sup>

Although ATN-DBS is effective in reducing seizures, the effect of ATN-DBS on ectopic granule cells and MFS in the chronic stage of epilepsy has not yet been investigated. Because of similar brain structures and circuits in humans and non-human primates, the non-human primate epileptic model seems to be most suitable for investigating the mechanism of ATN-DBS.<sup>[8,9]</sup> In this study, we used a kainic acid (KA)-induced epileptic model to investigate the effect of ATN-DBS on MFS, as well as potential signaling pathways.

## Methods

### Ethical approval

The experiments were performed under the guidelines for the use and care of experimental animals and the study was approved by the Ethics Committee of Beijing Neurosurgical Institute, Beijing, China (No. 201703002). All efforts were made to minimize animal suffering.

### Animals and grouping

Twenty-four male rhesus macaques (provided by the Animal Center of Military Medical Sciences, Beijing, China; age  $7.3 \pm 1.2$  years; weight  $8.3 \pm 1.4$  kg) were randomly divided into a control group ( $n = 6$ ), an epilepsy (EP) group ( $n = 6$ ), an EP-sham-DBS group ( $n = 6$ ), and an EP-DBS group ( $n = 6$ ). All the animals were kept in an environmentally controlled room ( $23\text{--}25^\circ\text{C}$ ; 12 h light/12 h dark cycle, lights on at 07:00), with free access to food and water.

### Establishment of epileptic model and behavior monitoring

The establishment of the epileptic model was described in our previous report.<sup>[10]</sup> Briefly, the monkeys were subjected to general anesthesia with an intramuscular injection of Zoletil (5 mg/kg; Virbac, Carros, France) and Dexdomitor (20  $\mu\text{g}/\text{kg}$ ; Zoetis, Parsippany, NJ, USA), before receiving a magnetic resonance imaging (MRI) scan using a 3-Tesla MRI scanner (Signa, GE Healthcare, Waukesha, WI, USA). KA (1  $\mu\text{g}/\mu\text{L}$ ; 1.5  $\mu\text{g}/\text{kg}/\text{target}$ ) was injected into the left hippocampus and amygdala in the epilepsy groups and normal saline (1.5  $\mu\text{L}/\text{kg}/\text{target}$ ) was injected at the same points in the control group. The surgical plan was based on pre-operative MRI scans and the injections were performed using the workstation of a neurosurgical robot system (RM-100, Beijing Baihui Weikang Technology Co., Ltd., Beijing, China). The vital signs of the animals were monitored throughout surgery.

Stereoelectroencephalography (SEEG) electrodes were implanted into the left hippocampus 24 h and 1 month after injection to detect epileptic discharge. The behavior of all animals was scored using the modified Racine scale: 0, no response; I, facial movement; II, head nodding and absence; III, unilateral forelimb clonus; IV, bilateral forelimb clonus and rearing; V, bilateral forelimb clonus, rearing, and falling.<sup>[10]</sup>

### ATN-DBS implantation and stimulation

Three weeks after the KA injection, monkeys in the EP-sham-DBS and EP-DBS groups underwent left ATN-DBS (L301; Beijing PINS Medical Co., Ltd., Beijing, China) implantation, based on the individuals' MRI scans and an atlas of the monkey brain.<sup>[11]</sup> An extension was tunneled subcutaneously through the neck to the abdomen, where an implantable pulse generator (G102, Beijing PINS Medical Co., Ltd.) was located. Post-operative computed tomography (CT) was performed to detect any complications and to confirm the accurate placement of the lead. One week after lead implantation, monkeys in the EP-DBS group were stimulated for 8 weeks (stimulation parameters: 1.5 V, 90  $\mu\text{s}$ , 150 Hz), and sites of stimulation contact were selected based on fused post-operative images. No electrical stimulation was delivered to animals in the EP-sham-DBS group.

### Tissue processing

Three months after the KA and normal saline injections, all monkeys were deeply anesthetized (20 mg/kg ketamine) and sacrificed. Three animals from each group were randomly selected for fresh tissue processing (subgroup A), and the left hippocampi were removed and stored at  $-80^\circ\text{C}$ . The remaining three monkeys in each group (subgroup B) were perfused with normal saline and then with 4% paraformaldehyde in 0.1 mol/L phosphate-buffered saline (PBS), before removing the brain [Figure 1A].

### Western blotting analysis

Brain tissues were washed with PBS and lysed in radio-immunoprecipitation assay buffer (50 mmol/L Tris-HCl [pH 7.4], 150 mmol/L sodium chloride, 1% Nonidet P-40, 0.1% sodium dodecyl sulfate [SDS]), containing phosphate and protease inhibitor cocktails. The homogenates were centrifuged at  $12,000 \times g$  for 20 min. The protein concentrations in the supernatants were determined using a bicinchoninic acid protein assay kit (Pierce, Rockford, IL, USA). Total protein (60  $\mu\text{g}$ ) was resolved by SDS-polyacrylamide gel electrophoresis on a 12% polyacrylamide gel and transferred to polyvinylidene difluoride membrane (Millipore, Billerica, MA, USA). The membranes were blocked with 10% milk for 1 h and then incubated with the following primary antibodies: rabbit anti- $\beta$ -actin (1:5000; Sigma-Aldrich, St. Louis, MO, USA, A5060), rabbit anti-phosphorylated (p)-Akt (1:1000, 4060S; Cell Signaling Technology, Danvers, MA, USA), rabbit anti-Akt (1:1000, 4691S; Cell Signaling Technology, Danvers, MA, USA), and rabbit anti-PKA (1:1000, LS-C63197-50; Lifespan Biosciences, Seattle, WA, USA). The membranes were then incubated with the secondary

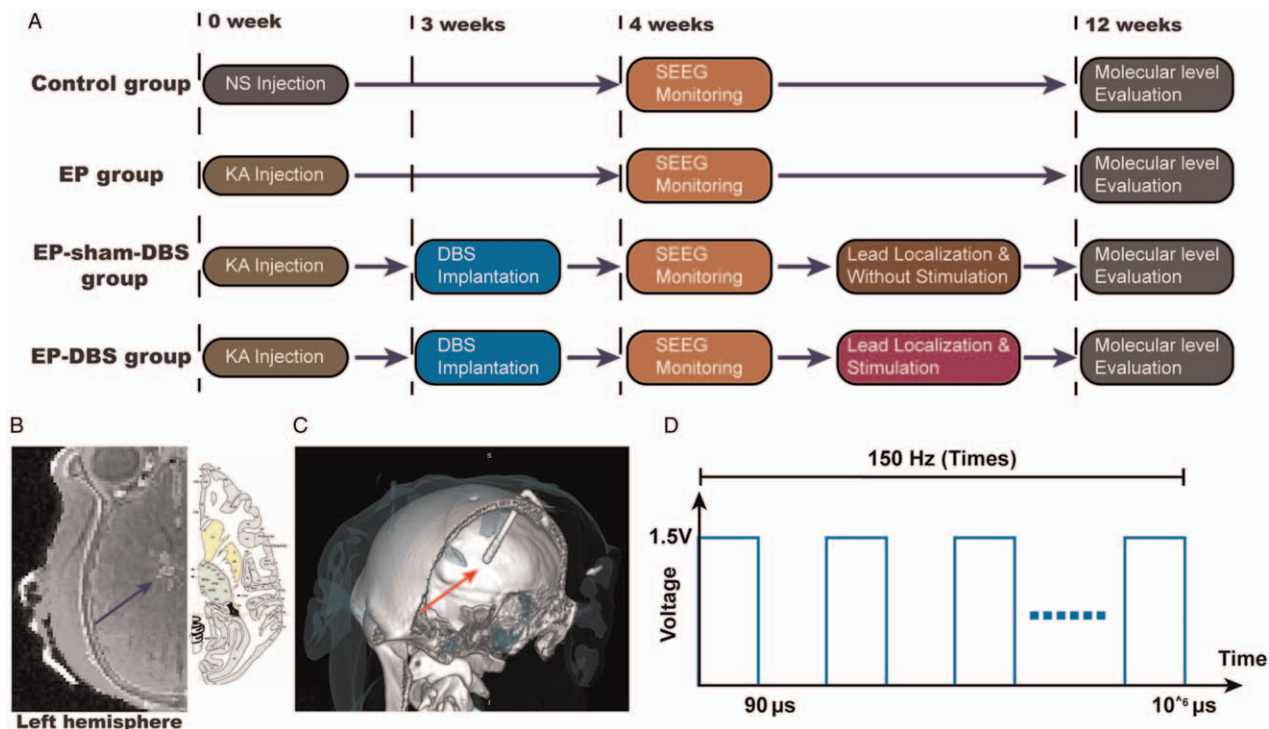


**Figure 1:** Flowchart showing the experimental design (A). Position of ATN-DBS. The DBS lead (arrow) was accurately targeted to the left of the ATN, by comparison with the atlas of the monkey brain (B).<sup>[11]</sup> 3D reconstruction of DBS lead (C). Stimulation parameters were set as 1.5 V, 90 μs, and 150 Hz. ATN-DBS, anterior thalamic nuclei deep brain stimulation (D). *n* = 6 in each group. ATN: Anterior thalamic nuclei; DBS: Deep brain stimulation; EP: Epilepsy; KA: Kainic acid; NS: Normal saline; SEEG: Stereoelectroencephalography.

antibody and the protein bands were visualized with enhanced chemiluminescence and quantified using ImageJ software. β-actin was used as the loading control.

**cAMP assay**

cAMP levels were measured using a cAMP Direct Immunoassay Kit (Abcam, Cambridge, MA, USA, ab65355), according to the manufacturer’s instructions. The kit contains a recombinant protein G-coated 96-well plate that facilitates the binding of a cAMP polyclonal antibody to the plate. cAMP-horseradish peroxidase (HRP) conjugate directly competes with cAMP in the sample for binding to cAMP antibody bound to the plate. After incubation and washing, the amount of cAMP-HRP bound to the plate can easily be determined using optical density at 450 nm to detect HRP activity. The optical density at 450 nm is inversely proportional to the concentration of cAMP in the sample. The concentration of cAMP in the test sample is calculated as  $cAMP \text{ concentration} = \frac{S_a}{S_v} * D$ , where *S<sub>a</sub>* is the amount of cAMP in the sample well, calculated from the standard curve (pmol/μL, nmol/mL, or μmol/L); *S<sub>v</sub>* is the sample volume added to the sample well (μL); and *D* is the sample dilution factor if the sample is diluted to fit within the standard curve range before the reaction well is set up.

**Immunofluorescence (IF) staining**

IF was performed as previously described.<sup>[3]</sup> Briefly, brain tissue sections were rinsed in PBS and permeabilized with 0.3% Triton X-100 in PBS for 30 min at room tempera-

ture. The sections were blocked with 10% normal goat serum for 1 h and then incubated overnight at 4°C with rabbit anti-NeuN (1:500; Abcam, Cambridge, MA, USA, ab128886) or mouse anti-Calbindin-D28k (1:1000, Sigma-Aldrich, St. Louis, MO, USA, C9848), followed by incubation with an Alexa Fluor 594- or 488-conjugated secondary antibody (1:500; Life Technologies, Waltham, Massachusetts, USA) for 1 h at room temperature. The cell nuclei were visualized by counterstaining them with 4',6-diamidino-2-phenylindole (Sigma-Aldrich). The sections were observed by confocal microscopy (LSM880, Zeiss, Germany).

Based on the atlas, three matched sections from each group were prepared for evaluation<sup>[11]</sup> and four views in each section were randomly selected for the measurement of ectopic granule cell numbers. MFS scores were measured in each section by two independent observers, based on the criteria presented in Tables 1 and 2.<sup>[12,13]</sup> Ectopic granule cell numbers and MFS scores were averaged for each monkey.

**Statistical analysis**

Data are expressed as means ± standard deviations. One-way analysis of variance followed by the Tukey *post hoc* correction was used to analyze the statistical significance of differences among multiple groups. Data were analyzed using SPSS 21.0 software (IBM, Chicago, IL, USA) and plotted using GraphPad Prism version 7.0 software (GraphPad Software, La Jolla, CA, USA). A *P* value < 0.05 was considered significant.

**Table 1: Mossy fiber scoring in the hippocampal CA3 subfield.**

Score	Description
0	No granules observed in stratum pyramidale or stratum oriens along the portion of the CA3 sub-region
1	Sparse granules present in discrete bundles
2	Moderate granules observed
3	Prominent granules observed
4	Prominent granules accompanied by near-continuous distribution observed along the entire CA3 region
5	Continuous or near-continuous dense laminar band of granules observed along the entire CA3 region

**Table 2: Mossy fiber scoring in the hippocampal dentate gyrus region.**

Score	Description
0	No granules between tips and crest
1	Sparse granules in the supragranular region in patchy distribution between tips and crest
2	More numerous granules in the supragranular region in continuous distribution between tips and crest
3	Prominent granules in the supragranular region in continuous pattern between tips and crest, with occasional patches of confluent granules between tips and crests
4	Prominent granules in the supragranular region forming confluent dense laminar band between tips and crest
5	Confluent dense laminar band of granules in the supragranular region extending into the inner molecular layer

## Results

### *ATN-DBS reduced seizure frequency in the chronic stage in epileptic monkeys*

A schematic showing the experimental design is provided in Figure 1A. The fusion of pre-operative MRI and post-operative CT images indicated accurate lead positions [Figures 1B and 1C]. Position errors were summarized in our previous study.<sup>[14]</sup> Status epilepticus was regarded as a single epileptic seizure lasting >5 min or two or more seizures within a 5-min period, without a return to normal between the seizures. No seizures were observed in the control group, whereas status epilepticus and recurrent spontaneous seizures were observed in all monkeys in the EP, EP-sham-DBS, and EP-DBS groups. The abnormal SEEG signal was reported in our previous study.<sup>[10]</sup>

Monkeys in the EP-DBS group received ATN stimulation and the total seizure number in this group was significantly reduced compared with the EP-sham-DBS and EP groups. Details were summarized in our previous study [Figure 1D].<sup>[15]</sup>

### *ATN-DBS decreased numbers of hilar ectopic granule cells in the chronic stage in epileptic monkeys*

Hilar ectopic granule cells are rare in normal adult animals, but, in the TLE model, numbers are greatly increased and this is closely associated with epileptogenesis.<sup>[6,16]</sup> NeuN is widely used as a marker of granule cells.<sup>[17]</sup> In animals with KA-induced epilepsy, there were significantly more NeuN-positive cells in the dentate hilus than those in the dentate hilus of control animals. ATN stimulation significantly reduced the number of NeuN-positive cells in the dentate hilus of the epileptic monkeys ( $F_{(3,8)} = 81.56$ ,  $P < 0.0001$ ), indicating that ATN-DBS reduces the number of hilar ectopic granule cells in the chronic stage in epileptic monkeys [Figures 2A and 2B].

### *ATN-DBS inhibited the cAMP/PKA signaling pathway in the hippocampus of epileptic monkeys*

cAMP, which activates PKA, has been shown to play an indispensable role in the progression of MFS.<sup>[5]</sup> In this study, a significant elevation of cAMP expression in the hippocampus was observed in the EP and EP-sham-DBS groups compared with the control group. This increase in cAMP expression was reversed in animals that received chronic ATN-DBS ( $F_{(3,8)} = 11.33$ ,  $P = 0.0030$ ) [Figure 3A]. A similar trend toward changing PKA expression was observed in these groups ( $F_{(3,8)} = 29.68$ ,  $P = 0.0001$ ) [Figures 3B and 3C]. The changes in cAMP and PKA expression suggest that ATN-DBS inhibits the cAMP/PKA signaling pathway in the chronic epileptic model.

### *ATN-DBS decreased Akt phosphorylation in the hippocampus of epileptic monkeys*

Akt phosphorylation, which is mediated by the cAMP/PKA signaling pathway, influences hippocampal synaptic plasticity.<sup>[18]</sup> Normal and low phosphorylated Akt/Akt was observed in the control group monkeys but the ratio was increased by KA injection in the epileptic model. Interestingly, a significant decrease in the ratio was observed in monkeys receiving ATN stimulation compared with the EP and EP-sham-DBS groups, as found in our previous study.<sup>[15]</sup>

### *ATN-DBS inhibited MFS in the dentate gyrus (DG) and CA3 regions of the chronic epileptic hippocampus*

Calbindin-D28k is a  $Ca^{2+}$ -binding protein that shows a characteristic spatial pattern of expression in the hippocampus and is a marker of the mossy fibers.<sup>[19]</sup> In the control group, no obvious calbindin-D28k granules were seen in the supragranular region of the DG or in

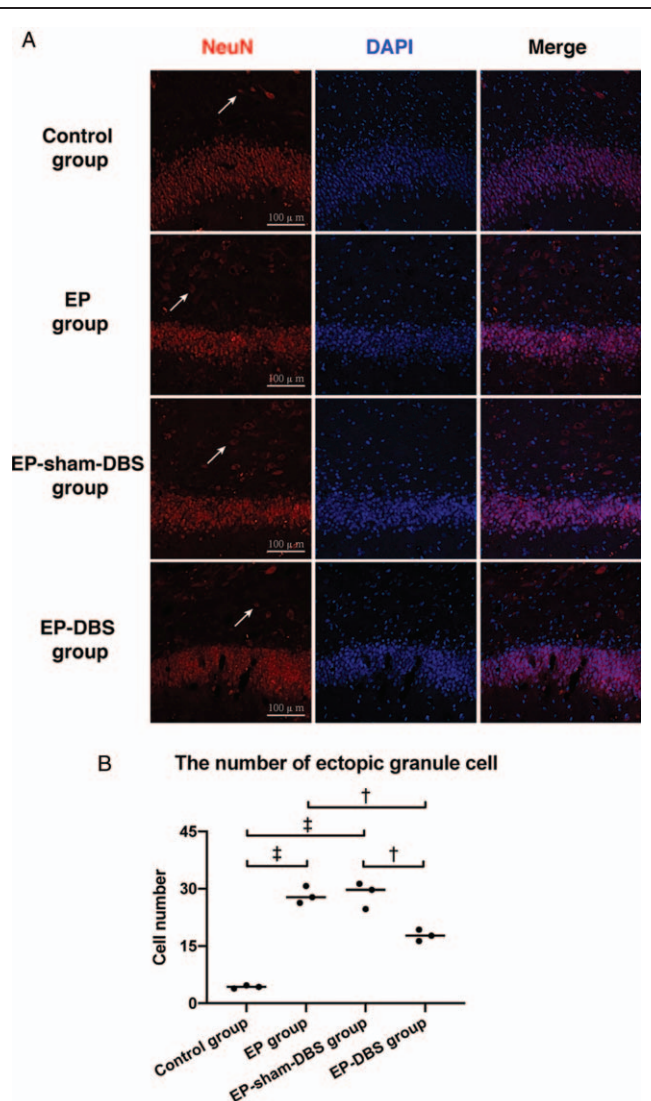


**Figure 2:** Number of hilar ectopic granule cells (arrows) in different groups (A, B). In the KA-induced epileptic model, the number of NeuN-positive cells in the dentate hilus in the EP and EP-sham-DBS groups was significantly increased compared with the control group and was significantly reduced in epileptic monkeys that received ATN stimulation. NeuN and DAPI were labeled as “red” and “blue,” respectively. <sup>†</sup> $P < 0.01$ ; <sup>‡</sup> $P < 0.001$ . ATN: Anterior thalamic nuclei; DAPI: 4',6-Diamidino-2-phenylindole; DBS: Deep brain stimulation; EP: Epilepsy; KA: Kainic acid; NeuN: Neuronal nuclei.

the pyramidal cell layer and stratum oriens of the CA3 region. In the EP and EP-sham-DBS groups, prominent MFS was observed in the inner molecular layer of the DG. In the CA3 region, calbindin-D28k staining was noted primarily in the pyramidal cell layer, with obvious MFS. Consistently, MFS scores in the DG and CA3 regions in the EP and EP-sham-DBS groups were significantly higher than those in the controls. In the EP-DBS group, less MFS was observed in the DG and CA3, with a significant decrease in MFS scores compared with the EP and EP-sham-DBS groups (CA3:  $F_{(3,8)} = 40.30$ ,  $P < 0.0001$ ; DG:  $F_{(3,8)} = 36.32$ ,  $P < 0.0001$ ) [Figure 4A–4D]. These results indicate that ATN-DBS inhibits MFS in the DG and CA3 regions in the chronic epileptic monkey model.

**Discussion**

ATN-DBS has been shown to have an ideal therapeutic effect in TLE,<sup>[4]</sup> and MFS plays an indispensable role in the pathogenesis and progression of TLE. Our previous study confirmed that ATN-DBS can inhibit MFS in the acute and latent stages in a rat model of TLE.<sup>[20]</sup> Clinically, most patients who receive ATN-DBS have suffered from epilepsy for several years, and sometimes for more than 10 years, which is regarded as the chronic stage of epilepsy. It was, however, not known whether ATN-DBS can inhibit MFS in the chronic stage of TLE and the potential pathways involved in any effect were also unknown. In this study, we showed that ATN-DBS inhibits MFS in chronic TLE, perhaps by reducing the number of ectopic granule cells and by modifying the cAMP/PKA signaling pathway [Figure 4E].

**MFS in TLE was inhibited by ATN-DBS**

Dentate granule cells project unmyelinated axons, such as mossy fibers, through the hippocampal dentate hilus to the CA3 region.<sup>[21]</sup> Under epileptic conditions, the mossy fiber collaterals robustly branch out of the hilus and aberrantly, or reversely, project to the inner third of the molecular layer, in which the mossy fibers form excitatory synapses, primarily on the granule cell dendrites.<sup>[22]</sup> MFS has also been reported to develop in the CA3 outside the stratum lucidum. MFS is a common pathological hallmark in

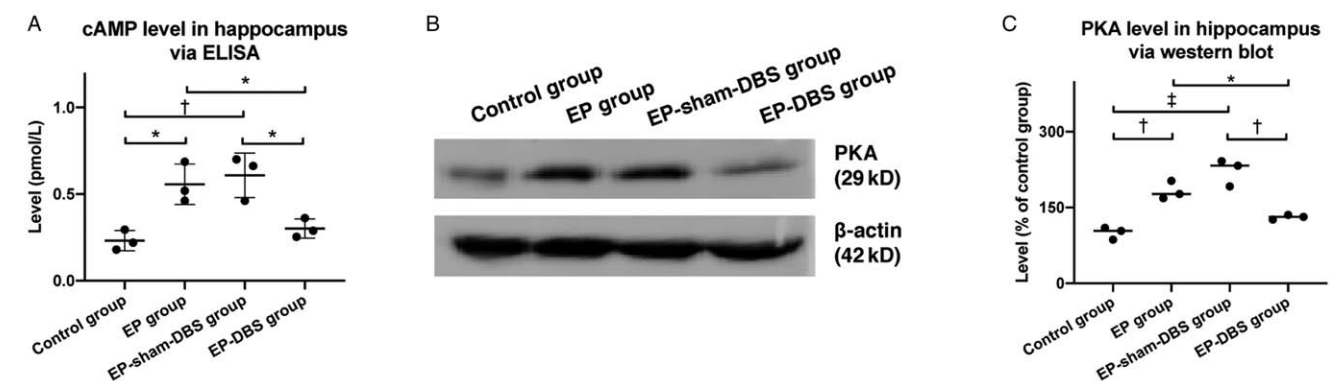


**Figure 3:** cAMP levels in the hippocampus. Significant down-regulation of cAMP expression was observed in the hippocampi of animals that received ATN-DBS (A). PKA levels in the hippocampus. Increased PKA expression was reversed in the EP-DBS group compared with the EP and EP-sham-DBS groups (B, C). <sup>\*</sup> $P < 0.05$ ; <sup>†</sup> $P < 0.01$ ; <sup>‡</sup> $P < 0.001$ . ATN: Anterior thalamic nuclei; cAMP: 3',5'-Cyclic adenosine monophosphate; DBS: Deep brain stimulation; ELISA: Enzyme-linked immunosorbent assay; EP: Epilepsy; PKA: Protein kinase A.

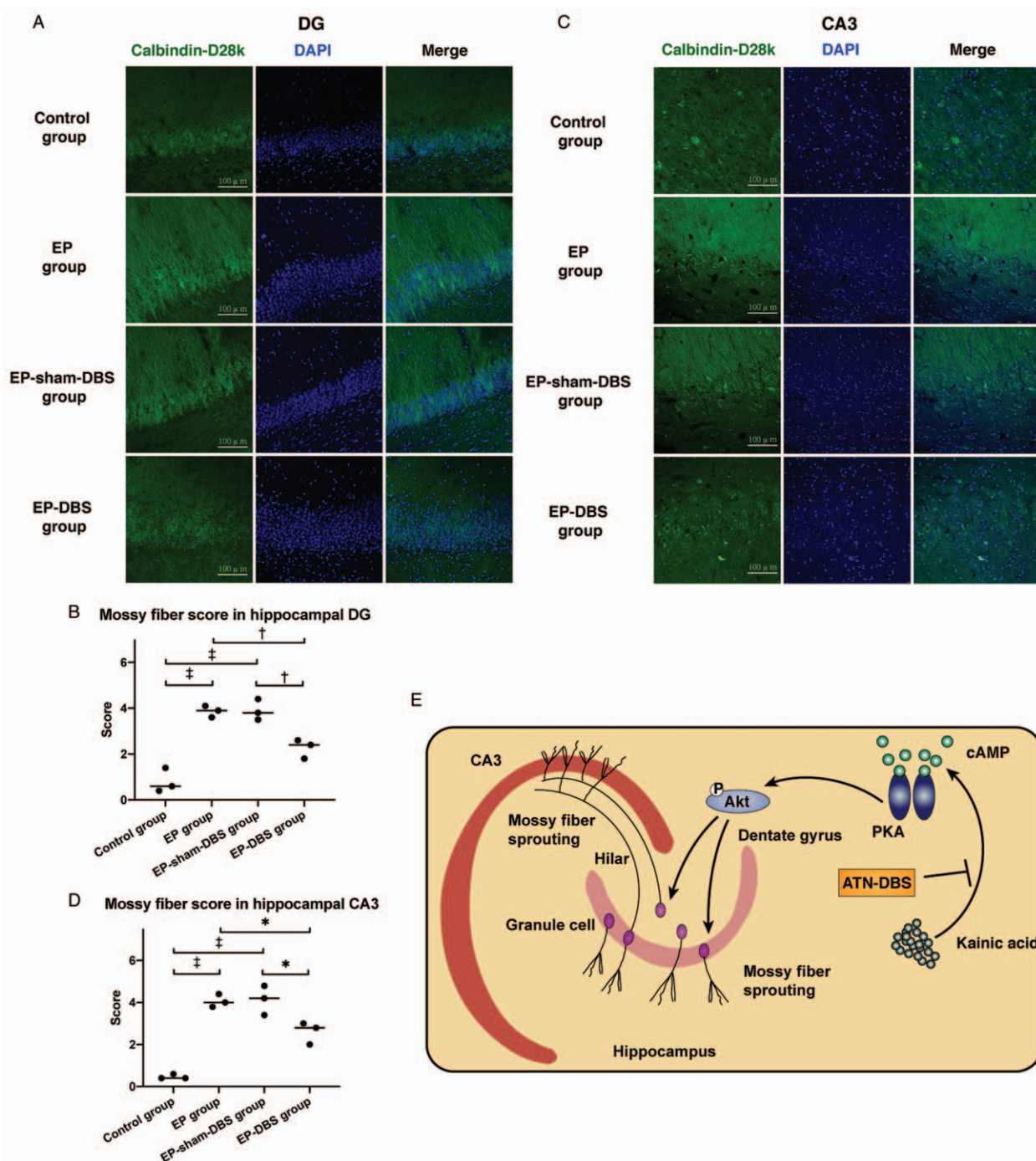


**Figure 4:** MFS in the DG and CA3. In the EP-DBS group, less MFS was observed in the DG and CA3 (A, C). MFS scores in the DG and CA3 regions. A significant decrease in MFS scores was observed in the EP-DBS group (B, D). Schematic illustration of the inhibitory effect of ATN-DBS on MFS in chronic epilepsy (E). Calbindin-D28k and DAPI were labeled as “green” and “blue,” respectively. \* $P < 0.05$ ; † $P < 0.01$ ; ‡ $P < 0.001$ . ATN: Anterior thalamic nuclei; cAMP: 3',5'-Cyclic adenosine monophosphate; DAPI: 4',6-Diamidino-2-phenylindole; DBS: Deep brain stimulation; DG: Dentate gyrus; EP: Epilepsy; MFS: Mossy fiber sprouting; PKA: Protein kinase A.

individuals with mesial TLE and the proportion of granule cells with sprouted mossy fibers has been estimated to be approximately 60%.<sup>[23]</sup>

Electron microscopy studies have shown that sprouted mossy fiber terminals form asymmetric (excitatory) contacts with the dendritic spines of granule cells.<sup>[24]</sup> Electrophysiological evidence was obtained using the perforant pathway stimulation (PPS). A single PPS in

hippocampal slices of normal rats was able to produce an excitatory postsynaptic potential (EPSP) and a population action potential in the granule cells. If a second PPS was triggered, it evoked the EPSP but not the population action potential. When the same experiment was performed in hippocampal slices of KA-treated rats, the second stimulation evoked multiple populations of action potentials, indicating that granule cells became disinhibited, and thus hyperexcitable. These observations were associated

with the presence of robust MFS in the hippocampal slices, suggesting that the aberrant sprouting of mossy fibers into the molecular layer was associated with the loss of the dentate “gate.”<sup>[25]</sup> In our study, we found that ATN-DBS can inhibit MFS in the chronic stage of epilepsy in the TLE monkey model. Considering the mechanism of MFS in TLE, it can be assumed that loss of the dentate “gate” is relieved by ATN-DBS. In our previous study, we demonstrated that ATN-DBS can reverse the increase in levels of the excitatory neurotransmitter glutamate,<sup>[7]</sup> which may contribute to the inhibition of MFS, complementing the findings of this study.

### **MFS is associated with ectopic granule cells and cAMP/PKA signaling pathway, which is reversed by ATN-DBS**

There are two locations in the adult mammalian brain where new neurons are generated throughout life. One is the subventricular zone and the other is the DG.<sup>[26]</sup> In the normal brain, adult-born progenitors appear to have sufficient intrinsic programming and adequate extrinsic cues to develop and migrate normally, with ectopic granule cells appearing rarely.<sup>[6]</sup> Previous studies that focused on the hilus, however, showed that ectopic granule cells induced by either pilocarpine or KA in adult rats or mice survive long-term, at least 18 months.<sup>[6,27]</sup> Remarkably, ectopic granule cells appear to have mossy fiber axons that are extremely similar to those of granule cells in the epileptic rat. All of the ectopic granule cells that have been examined had collaterals in the hilus and projected into the stratum lucidum of area CA3.<sup>[6]</sup> In this study, a substantially larger number of ectopic granule cells was observed in the chronic epileptic monkey. Chronic ATN-DBS significantly reversed this trend, indicating that ATN-DBS inhibits the development of ectopic granule cells.

The cellular process of MFS has been proposed to follow a three-step axon guidance model: step 1, branching; step 2, reverse projection; and step 3, fasciculation. It has been further suggested that this processing could be regulated by specific signaling pathways.<sup>[5]</sup> Axonal branching is partly mediated by cAMP<sup>[28]</sup> and a previous study, using an optogenetic method to photoactivate primary cultures of granule cells expressing photoactivated adenylyl cyclase, showed that activity-dependent increases in intracellular cAMP levels alone could induce mossy fiber branching.<sup>[29]</sup> In mice lacking adenylyl cyclase 8 (which catalyzes the synthesis of cAMP from ATP), MFS in the DG area was also decreased following the injection of pilocarpine.<sup>[30]</sup> Agents that elevate cAMP levels could activate Akt through PKA, and a trend of Akt was confirmed. Pre-treatment with perifosine, an inhibitor of Akt, suppressed KA-induced neuronal death and MFS.<sup>[31]</sup> The frequency of spontaneous seizures was also markedly reduced in rats pre-treated with perifosine.<sup>[31]</sup> Mycophenolate mofetil, which is commonly used as an immunosuppressant in organ transplantations, reduces MFS in the DG and CA3 regions of the hippocampus, possibly via the Akt signaling pathway.<sup>[32]</sup>

In conclusion, ATN-DBS was shown to down-regulate the cAMP/PKA signaling pathway and Akt phosphorylation

and to reduce the number of ectopic granule cells, which may contribute to the inhibition of MFS of chronic TLE. Our study provides further insights into the mechanism by which ATN-DBS reduces epileptic seizures.

### **Funding**

This study was supported by the National Nature Science Foundation of China (Nos. 81671104, 81701268, 61761166004, and 81830033), the Beijing Municipal Administration of Hospitals' Ascent Plan (No. DFL20150503), the Capital Health Research and Development of Special (No. 2018-2-1076), and the China Postdoctoral Science Foundation (No. 2018T110120).

### **Conflicts of interest**

None.

### **References**

1. Benbadis SR, Allen Hauser W. An estimate of the prevalence of psychogenic non-epileptic seizures. *Seizure* 2000;9:280–281. doi: 10.1053/seiz.2000.0409.
2. Malerba A, Ciampa C, De Fazio S, Fattore C, Frassine B, La Neve A, et al. Patterns of prescription of antiepileptic drugs in patients with refractory epilepsy at tertiary referral centres in Italy. *Epilepsy Res* 2010;91:273–282. doi: 10.1016/j.epilepsyres.2010.08.002.
3. Chen YC, Zhu GY, Wang X, Shi L, Jiang Y, Zhang X, et al. Deep brain stimulation of the anterior nucleus of the thalamus reverses the gene expression of cytokines and their receptors as well as neuronal degeneration in epileptic rats. *Brain Res* 2017;1657:304–311. doi: 10.1016/j.brainres.2016.12.020.
4. Salanova V, Witt T, Worth R, Henry TR, Gross RE, Nazzaro JM, et al. Long-term efficacy and safety of thalamic stimulation for drug-resistant partial epilepsy. *Neurology* 2015;84:1017–1025. doi: 10.1212/wnl.0000000000001334.
5. Koyama R, Ikegaya Y. The molecular and cellular mechanisms of axon guidance in mossy fiber sprouting. *Front Neurol* 2018;9:382. doi: 10.3389/fneur.2018.00382.
6. Scharfman HE, Pierce JP. New insights into the role of hilar ectopic granule cells in the dentate gyrus based on quantitative anatomic analysis and three-dimensional reconstruction. *Epilepsia* 2012;53:109–115. doi: 10.1111/j.1528-1167.2012.03480.x.
7. Shi L, Yang AC, Li JJ, Meng DW, Jiang B, Zhang JG. Favorable modulation in neurotransmitters: effects of chronic anterior thalamic nuclei stimulation observed in epileptic monkeys. *Exp Neurol* 2015;265:94–101. doi: 10.1016/j.expneurol.2015.01.003.
8. Charvet CJ, Finlay BL. Comparing adult hippocampal neurogenesis across species: translating time to predict the tempo in humans. *Front Neurosci* 2018;12:706. doi: 10.3389/fnins.2018.00706.
9. Seress L. Morphological variability and developmental aspects of monkey and human granule cells—differences between the rodent and primate dentate gyrus. *Epilepsy Res* 1992;7:3–28. doi: 10.1111/j.1528-1157.1992.tb05897.x.
10. Chen Y, Zhu G, Shi L, Liu D, Zhang X, Liu Y, et al. Establishment of a novel mesial temporal lobe epilepsy rhesus monkey model via intra-hippocampal and intra-amygdala kainic acid injection assisted by neurosurgical robot system. *Brain Res Bull* 2019;149:32–41. doi: 10.1016/j.brainresbull.2019.04.002.
11. Saleem KS, Logothetis NK. A Combined MRI and Histology Atlas of the Rhesus Monkey Brain in Stereotaxic Coordinates. Amsterdam, The Netherlands: Academic Press; 2007.
12. Cavazos JE, Golarai G, Sutula TP. Septotemporal variation of the supragranular projection of the mossy fiber pathway in the dentate gyrus of normal and kindled rats. *Hippocampus* 1992;2:363–372. doi: 10.1002/hipo.450020404.
13. Lin W, Huang W, Chen S, Lin M, Huang Q, Huang H. The role of 5-HTR6 in mossy fiber sprouting: activating Fyn and p-ERK1/2 in pilocarpine-induced chronic epileptic rats. *Cell Physiol Biochem* 2017;42:231–241. doi: 10.1159/000477322.

14. Zhu GY, Chen YC, Du TT, Liu DF, Zhang X, Liu YY, *et al.* The accuracy and feasibility of robotic assisted lead implantation in nonhuman primates. *Neuromodulation* 2019;22:441–450. doi: 10.1111/ner.12951.
15. Du TT, Zhu G, Chen Y, Shi L, Liu D, Liu Y, *et al.* Anterior thalamic nucleus stimulation protects hippocampal neurons by activating autophagy in epileptic monkeys. *Aging (Albany NY)* 2020;12:6324–6339. doi: 10.18632/aging.103026.
16. Sugaya Y, Maru E, Kudo K, Shibasaki T, Kato N. Levetiracetam suppresses development of spontaneous EEG seizures and aberrant neurogenesis following kainate-induced status epilepticus. *Brain Res* 2010;1352:187–199. doi: 10.1016/j.brainres.2010.06.061.
17. Pun RYK, Rolfe IJ, LaSarge CL, Hosford BE, Rosen JM, Uhl JD, *et al.* Excessive activation of mTOR in postnatally generated granule cells is sufficient to cause epilepsy. *Neuron* 2012;75:1022–1034. doi: 10.1016/j.neuron.2012.08.002.
18. Spencer-Segal JL, Tsuda MC, Mattei L, Waters EM, Romeo RD, Milner TA, *et al.* Estradiol acts via estrogen receptors alpha and beta on pathways important for synaptic plasticity in the mouse hippocampal formation. *Neuroscience* 2012;202:131–146. doi: 10.1016/j.neuroscience.2011.11.035.
19. Rami A, Niquet J, Konoplev A. Early aberrant growth of mossy fibers after status epilepticus in the immature rat brain. *Mol Neurobiol* 2019;56:5025–5031. doi: 10.1007/s12035-018-1432-y.
20. Zhu G, Meng D, Chen Y, Du T, Liu Y, Liu D, *et al.* Anterior nucleus of thalamus stimulation inhibited abnormal mossy fiber sprouting in kainic acid-induced epileptic rats. *Brain Res* 2018;1701:28–35. doi: 10.1016/j.brainres.2018.07.014.
21. Amaral DG, Scharfman HE, Lavenex P. The dentate gyrus: fundamental neuroanatomical organization (dentate gyrus for dummies). *Prog Brain Res* 2007;163:3–22. doi: 10.1016/S0079-6123(07)63001-5.
22. Buckmaster PS, Zhang GF, Yamawaki R. Axon sprouting in a model of temporal lobe epilepsy creates a predominantly excitatory feedback circuit. *J Neurosci* 2002;22:6650–6658. doi: 10.1523/JNEUROSCI.22-15-06650.2002.
23. Isokawa M, Levesque MF, Babb TL, Engel J. Single mossy fiber axonal systems of human dentate granule cells studied in hippocampal slices from patients with temporal lobe epilepsy. *J Neurosci* 1993;13:1511–1522. doi: 10.1523/JNEUROSCI.13-04-01511.1993.
24. Represa A, Jorquera I, Le Gal La Salle G, Ben-Ari Y. Epilepsy induced collateral sprouting of hippocampal mossy fibers: does it induce the development of ectopic synapses with granule cell dendrites? *Hippocampus* 1993;3:257–268. doi: 10.1002/hipo.450030303.
25. Cavarsan CF, Malheiros JM, Hamani C, Najm IM, Covolan L. Is the mossy fiber sprouting a potential therapeutic target for epilepsy? *Front Neurol* 2018;9:1023. doi: 10.3389/fneur.2018.01023.
26. Bergmann O, Spalding KL, Frisén J. Adult neurogenesis in humans. *Cold Spring Harb Perspect Biol* 2015;7:a018994. doi: 10.1101/cshperspect.a018994.
27. Jessberger S, Zhao C, Toni N, Clemenson GD Jr, Li Y, Gage FH. Seizure-associated, aberrant neurogenesis in adult rats characterized with retrovirus-mediated cell labeling. *J Neurosci* 2007;27:9400–9407. doi: 10.1523/JNEUROSCI.2002-07.2007.
28. Mingorance-Le Meur A, O'Connor TP. Neurite consolidation is an active process requiring constant repression of protrusive activity. *EMBO J* 2009;28:248–260. doi: 10.1038/emboj.2008.265.
29. Zhou X, Tanaka KF, Matsunaga S, Iseki M, Watanabe M, Matsuki N, *et al.* Photoactivated adenylyl cyclase (PAC) reveals novel mechanisms underlying cAMP-dependent axonal morphogenesis. *Sci Rep* 2016;5:19679. doi: 10.1038/srep19679.
30. Chen X, Dong G, Zheng C, Wang H, Yun W, Zhou X. A reduced susceptibility to chemoconvulsant stimulation in adenylyl cyclase 8 knockout mice. *Epilepsy Res* 2016;119:24–29. doi: 10.1016/j.eplepsyres.2015.11.007.
31. Zhu F, Kai J, Chen L, Wu M, Dong J, Wang Q, *et al.* Akt inhibitor perifosine prevents epileptogenesis in a rat model of temporal lobe epilepsy. *Neurosci Bull* 2018;34:283–290. doi: 10.1007/s12264-017-0165-7.
32. Mazumder AG, Patial V, Singh D. Mycophenolate mofetil contributes to downregulation of the hippocampal interleukin type 2 and 1beta mediated PI3K/AKT/mTOR pathway hyperactivation and attenuates neurobehavioral comorbidities in a rat model of temporal lobe epilepsy. *Brain Behav Immun* 2019;75:84–93. doi: 10.1016/j.bbi.2018.09.020.

---

**How to cite this article:** Du TT, Chen YC, Zhu GY, Liu DF, Liu YY, Yuan TS, Zhang X, Zhang JG. Anterior thalamic nuclei deep brain stimulation inhibits mossy fiber sprouting via 3',5'-cyclic adenosine monophosphate/protein kinase A signaling pathway in a chronic epileptic monkey model. *Chin Med J* 2021;134:326–333. doi: 10.1097/CM9.0000000000001302